RESEARCH ARTICLE

Oxidation of lactate to pyruvate mediates the cytotoxic potential of physical plasma-treated saline solutions in ovarian cancer

Cristiana Bucci[1,2,3,4] | Francesco Tampieri[5,6,7] | Miguel Mateu-Sanz[5,6,7] | Romolo Laurita[3,4,8] | Vittorio Colombo[3,4,8,9] | Cristina Canal[5,6,7]

[1]Department of Medical and Surgical Sciences, Alma Mater Studiorum-University of Bologna, Bologna, Italy

[2]Department of Pharmacy and Biotechnology, Alma Mater Studiorum-University of Bologna, Bologna, Italy

[3]Department of Industrial Engineering, Alma Mater Studiorum-University of Bologna, Bologna, Italy

[4]Centro di Studio e Ricerca sulle Neoplasie Ginecologiche, Alma Mater Studiorum-University of Bologna, Bologna, Italy

[5]Biomaterials, Biomechanics and Tissue Engineering Group, Materials Science and Engineering Department and Research Center for Biomedical Engineering, Universitat Politècnica de Catalunya·Barcelonatech (UPC), Barcelona, Spain

[6]Barcelona Research Center in Multiscale Science and Engineering, UPC, Barcelona, Spain

[7]Institut de Recerca Sant Joan de Déu, Barcelona, Spain

[8]Interdepartmental Center for Industrial Research Advanced Mechanical Engineering Applications and Materials Technology, Alma Mater Studiorum-University of Bologna, Bologna, Italy

Abstract

Epithelial ovarian cancer (EOC) is the most common type of gynecological tumor, presenting poor prognosis at diagnosis and with recurrences being frequently observed. Reactive species generated by physical plasma and transferred into liquids have shown promising results in cancer therapy. Recently, Ringer's lactate solution was exposed to plasma showing selective anticancer activity on EOC cells. In this work, we compared the effect of plasma treatment, using the kINPen plasma jet, on Ringer's saline and Ringer's lactate solution. These two plasma-treated liquids were analyzed chemically by quantifying reactive species and the extent of lactate oxidation. The biological efficiency of the plasma-treated liquids was explored in EOC cells. The results show that lactate is affected by plasma treatment, displaying a reduction of cytotoxic potential.
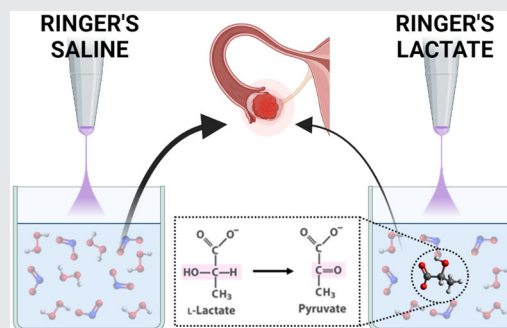
KEYWORDS

cold atmospheric plasma, epithelial ovarian cancer, kINPen, plasma-treated liquid, reactive species, Ringer's lactate, Ringer's saline

---

---

[9]Interdepartmental Center for Industrial Research Agrifood, Alma Mater Studiorum-University of Bologna, Bologna, Italy

Correspondence
Cristina Canal, Universitat Politècnica de Catalunya·Barcelonatech (UPC), c/Eduard Maristany 14, Barcelona 08019, Spain.
Email: cristina.canal@upc.edu

1 | INTRODUCTION

Epithelial ovarian cancer (EOC) is the most common gynecological malignant tumor, accounting for 90% of women's cancers.[1] It is characterized by neoplastic nodules located on the peritoneal surface with a mainly asymptomatic progression, with diagnosis in advanced stages in about 75% of cases.[1–3] Standard of care in advanced EOC is the combination of primary debulking surgery followed by platinum-taxane chemotherapy.[4,5] Even though chemotherapeutic approaches are an effective and tolerable way to treat many types of tumors, they still face many challenges, such as unspecific side-effect profiles that are still reported.[6,7] Despite improved survival rates,[8] conventional therapies cannot eradicate the disease[5,9] and about 80% of affected women relapse[10] with a poor prognosis in EOC advanced stages within 5 years from diagnosis.[4,11] Hence, innovative and adjuvant solutions have to be found to improve EOC therapy. Within this framework, cold atmospheric plasma (CAP) could be a promising approach.

CAP is a partially ionized gas characterized by a blend of neutral species (atoms, molecules, and radical species), charged particles (electrons, positive and negative ions) and electromagnetic radiation.[12,13] Consequently, plasma has a complex composition that has been widely explored in the field of plasma medicine for its therapeutic application.[12,14,15] CAP interaction with ambient air (oxygen and nitrogen) and water vapor allows the production of reactive oxygen and nitrogen species (RONS)[12] that may trigger cell death mechanisms and therefore find application in anticancer therapy.[16,17] Several in vitro and in vivo studies reported that cancer cells show sensitivity to CAP both when they are directly in contact with it and when they are exposed to CAP-treated solutions, also known as plasma-treated liquids (PTLs) that operate as donors of RONS.[13,18–21] Thereby, the short-lived RONS generated by CAP can diffuse into the liquid and react to form long-lived species, including nitrite ions (NO_2^-), generated by reactions of nitric oxide and nitrogen dioxide in water and hydrogen peroxides (H_2O_2), obtained by recombination of hydroxyl radicals (OH).[13,22–24] These latter species have a significant role in cellular biochemistry due to their influence on redox balance.[25–27] In fact, RONS, or derived species, play a pivotal role, being both proliferative and harmful signaling molecules, depending on their concentration and subcellular localization.[28–30] Under resting conditions, cells produce RONS as metabolic by-products that are detoxified by the antioxidant defenses to preserve cell survival and proliferation.[31] This strategy is particularly efficient in cancer cells, displaying high levels of antioxidant proteins to maintain their redox homeostasis but they still contain higher levels of RONS than non malignant cells.[25,32] Nevertheless, when the intracellular level of RONS exceeds a cell-specific threshold, antioxidant mechanisms fail to preserve cell survival leading to apoptosis.[17,31,33] In this perspective, the increase of oxidative stress in cancer cells caused by exogenous RONS may be a novel strategy to aid conventional cancer therapies.[32,34]

PTLs offer several advantages in clinical application, such as non invasiveness, modulation of long-lived reactive species rates such as H_2O_2 and, in some cases, possibility of storage, from days to months, without affecting the RONS content activity.[29,35–37] However, the prospect of applying PTLs in the clinical field requires selecting liquids suitable for medical applications, such as saline solutions. Several solutions have been exposed to CAP for cell treatments,[29,37–39] exhibiting antitumor activity against various types of cancer cells.[13,19,21,40,41] In particular, the exposure of physiological Ringer's lactate (RL) solution to CAP resulted in the production of plasma-treated Ringer's lactate (PTRL), which showed a cytotoxic effect on EOC while their healthy counterparts retained high survival.[32] Along that, the cytotoxic effect ascribed to another clinically suitable

solution, that is, Ringer's saline (R), on osteosarcoma was established,[39] which also showed a synergistic effect with doxorubicin and compromised metastatic potential[42] but has not been investigated for EOC. Both RL and R solutions are isotonic fluids whose simple composition has been used in hospitals and healthcare settings. They share the same basic composition (NaCl, KCl, and CaCl$_2$), although RL also contains lactate, in the form of sodium salt.[43] Lactate is a by-product of glucose metabolism during cell anaerobic phase, a cell state which requires an increase in energy demand.[44] During their life cycle, cells go through aerobic and anaerobic phases, which cause the continuous pyruvate oxidation–reduction in lactate to maintain a balanced energy ratio.[45] When lactate is oxidized to pyruvate, it contributes to the maintenance of glycolytic flux and acts, in turn, as a buffer system.[44,46,47] Understanding the mechanism leading to PTLs cytotoxicity is important to propose their use in the clinical field. Indeed, it was reported that organic elements as cell culture medium components may influence the CAP final biological effect, especially pyruvate, which has been reported to mitigate PTL efficiency given to its H$_2$O$_2$ scavenging activity.[48,49]

This work aims at investigating the lactate-mediated biological efficiency of physical plasma-treated saline solutions in ovarian cancer. Thus, Ringer's lactate and Ringer's saline solutions were exposed to kINPen plasma jet for several treatment times to produce PTRL and plasma-treated Ringer's saline (PTR), respectively. RONS generated by plasma in R and RL were quantified by colorimetric methods and the direct effect of plasma on lactate was studied by chromatography coupled with UV detection. Moreover, PTRL and PTR cytotoxicity was examined for the first time on four different EOC cell lines, pointing out the influence of lactate on the biological effect of PTLs.

2 | EXPERIMENTAL SECTION

2.1 | Atmospheric pressure plasma jet

PTLs were produced by exposing liquids to a commercial plasma jet (kINPen® IND, Neoplas tools GmbH).[50] The plasma device consists of a handheld unit that generates plasma under atmospheric conditions, driven by an AC power supply with 1 MHz frequency. It is composed of a pin-type powered electrode in a dielectric ceramic tube with a grounded outer electrode. Argon gas (Ar 5.0, Praxair) was used as a feed gas with a flow rate of 3 L/min. The plasma was operated at 10 mm distance from the nozzle to the surface of the liquid. The electrical and thermal characterization of the kINPen and the main excited species generated in the gas phase, analyzed by

optical emission spectroscopy, using the same experimental conditions reported in this manuscript, are reported by Mateu-Sanz et al. and Reuter et al.[39,50]

2.2 | PTL production and characterization

To obtain PTR and PTRL solutions, 1 mL of sterile R solution (102.7 mM NaCl, 5.4 mM KCl, and 1.8 mM CaCl$_2$·2H$_2$O) or RL solution (same composition of R plus the addition of 28.3 mM lactate, purchased by Fresenius Kabi) was placed in a 24-well plate and exposed to plasma treatment for selected times, in the range 15−300 s.

To isolate the effect of plasma treatment on lactate and to assess if the presence of lactate may influence the cell viability response, a solution of PTR to which 56.6 mM of L,—double the concentration than in the commercial RL solution—was added after the treatment (PTR+L) was used as a control.

The quantification of H$_2$O$_2$ and NO$_2^-$ generated during plasma treatment was performed using colorimetric chemical probes. H$_2$O$_2$ detection was carried out using the titanium(IV) oxysulfate method.[51] In the presence of hydrogen peroxide, Ti(IV) in sulfuric acid solution generates a yellow complex with absorption maximum at 410 nm. 50 µL of Ti(IV) oxysulfate solution was added to 100 µL of PTR or PTRL solution in a 96-well plate and the absorption spectra were recorded between 340 and 600 nm. NO$_2^-$ detection was carried out using Griess reagent (composed of 1% sulfanilamide, 0.1% N-(1-naphthyl) ethylene diamine, and 1.2% phosphoric acid in ultrapure water). 50 µL of Griess reagent was mixed with 50 µL of plasma-treated solution in a 96-well plate and the absorption spectra were recorded between 400 and 700 nm.[52] Calibration lines were built using standard solutions of hydrogen peroxide and sodium nitrite prepared in the same media used during plasma treatment.

Before and after each plasma treatment, the pH of the solutions was evaluated by using a MM 41 Crison multimeter. The production of hydroxyl radicals during the plasma treatment was studied using coumarin (COU).[53,54] COU reacts with free OH radicals to generate the fluorescent product 7-hydroxycoumarin (7-COU-OH), which can be used as an indirect measure of the amount of OH radicals generated by plasma treatment and transferred into the liquid. 1 mM solutions of COU in R and RL were treated with plasma using the conditions described above. After treatment, 400 µL was transferred in a 48-well plate and fluorescence was measured ($\lambda_{ex/em} = 360/460$ nm). Absorption and

fluorescence measurements were done using a Synergy HTX Hybrid Multi-Mode Microplate Reader (BioTek Instruments, Inc.). All measurements were done at least in triplicate. While it is known that the fluorescence of 7-COU-OH is pH sensitive, under certain conditions (the pH and excitation wavelengths used in this work) it can be considered negligible and it can safely be assumed that the change in fluorescence intensity observed during the experiments is mainly due to a higher production of hydroxyl-coumarin and not due to pH effects.

2.3 | High-performance liquid chromatography (HPLC) analysis of plasma-treated Ringer's lactate

HPLC coupled with diode array detector (DAD) was used to detect and quantify the residual lactate in the PTL samples and to verify the formation of oxidation products. The samples were diluted in R when necessary.

HPLC/DAD measurements were done using a Shimadzu Prominence XR instrument with LC-20AD XR pump, DGU-20A5R degassing unit, SIL-20AC HT autosampler and SPD-M20A UV/VIS photodiode array detector equipped with an Agilent Zorbax Sb-AQ analytical column ($3.5\,\mu m$, $4.6 \times 150\,mm$). Eluents were phosphate buffer 20 mM pH 1.5 (A, 16.3 mM H_3PO_4 + 3.7 mM $H_2PO_4^-$) and acetonitrile (B). Elution was isocratic (A:B 99:1), the flow rate was 1 mL/min, injection volume was $20\,\mu L$, temperature of the column and detector was 35°C, and detection was 190–400 nm. Under these conditions, the retention time (r.t.) for lactate was 2.47 min. The calibration lines for lactate and pyruvate were obtained by analyzing, under the same conditions, standard solutions in R. The areas of the peaks in the chromatograms were obtained, using the OriginPro 2020 software (version 9.7.0.188, OriginLab Corporation) after proper subtraction of the baseline and deconvolution, when necessary.

2.4 | Cell lines and culture conditions

Four human EOC cell lines, SKOV-3, OV-90, OVSAHO and OC314 (ATCC), were grown in Roswell Park Memorial Institute 1640 medium (RPMI 1640; Gibco™) supplemented with 10% fetal bovine serum (FBS), 2 mM L-glutamine, 100 U/mL penicillin and 100 µg/mL strepto-mycin (Gibco™). The cells were maintained in an incubator with a humidified atmosphere and 5% CO_2 at 37°C.

2.5 | Cell treatment and viability assay

EOC cells were seeded in 96-well plates in complete medium at a density of 3.5×10 cells/well, except OVSAHO cells which were cultured at 6×10^3 cells/well. After 24 h, cells were treated with $100\,\mu L$ of freshly produced PTRL, PTR, PTR+L or their corresponding untreated controls (UTs) for 2 h. Ten percent of heat-inactivated FBS was added to PTLs and PTRL (and to their UTs) to restore a physiological pH.[39] A previous work showed a mild H_2O_2 scavenging effect of FBS, which was more marked within 2–3 days after the treatment.[55] For this reason, the PTLs were used immediately after their production.

Afterward, cells were washed in phosphate-buffered saline (PBS) solution and cultured in complete medium at 37°C and 5% CO_2.

Cell viability was assayed using WST-1 assay (Roche) at 2, 24, and 72 h after treatment. Treated cell viability was assessed using $18\,\mu L/mL$ cell proliferation reagent WST-1 in supplemented RPMI (final volume per well $250\,\mu L$) and incubated for 1 h at 37°C. Afterward, $100\,\mu L$ of the supernatant was transferred to another well for absorbance measurement at 440 nm by using the microplate reader. The percentage of viability was calculated considering UT at 2 h as 100%.

2.6 | Colony formation assay

Colony formation assay was carried out by seeding SKOV-3 and OC314 in 6-well plates at low density (2×10^3 cells/well) in complete medium (Figure 1a,b).

To assess the cell clonogenicity, EOC cells were treated after 24 h of seeding; to assess the colony proliferative potential, EOC cells were cultured for 6 days, allowing them to form visible colonies, upon which they were treated. The treatments consisted of 2 mL/well of PTRL and PTR solution freshly produced at 15 and 20 s of plasma treatment time; after 2 h of incubation, cells were washed with PBS and cultured for 6 and 4 days additional at 37°C and 5% CO_2, respectively. As control, cells were exposed to 2 mL/well of untreated R or RL, both supplemented with 10% FBS. The medium was changed every 3 days.

Subsequently, colonies were fixed and stained with 80% crystal violet (CV) solution and 20% methanol for 20 min and washed five times with distilled water. Afterward, CV was dissolved in $10\%_{v/v}$ acetic acid and absorbance at 590 nm was measured using the micro-plate reader.
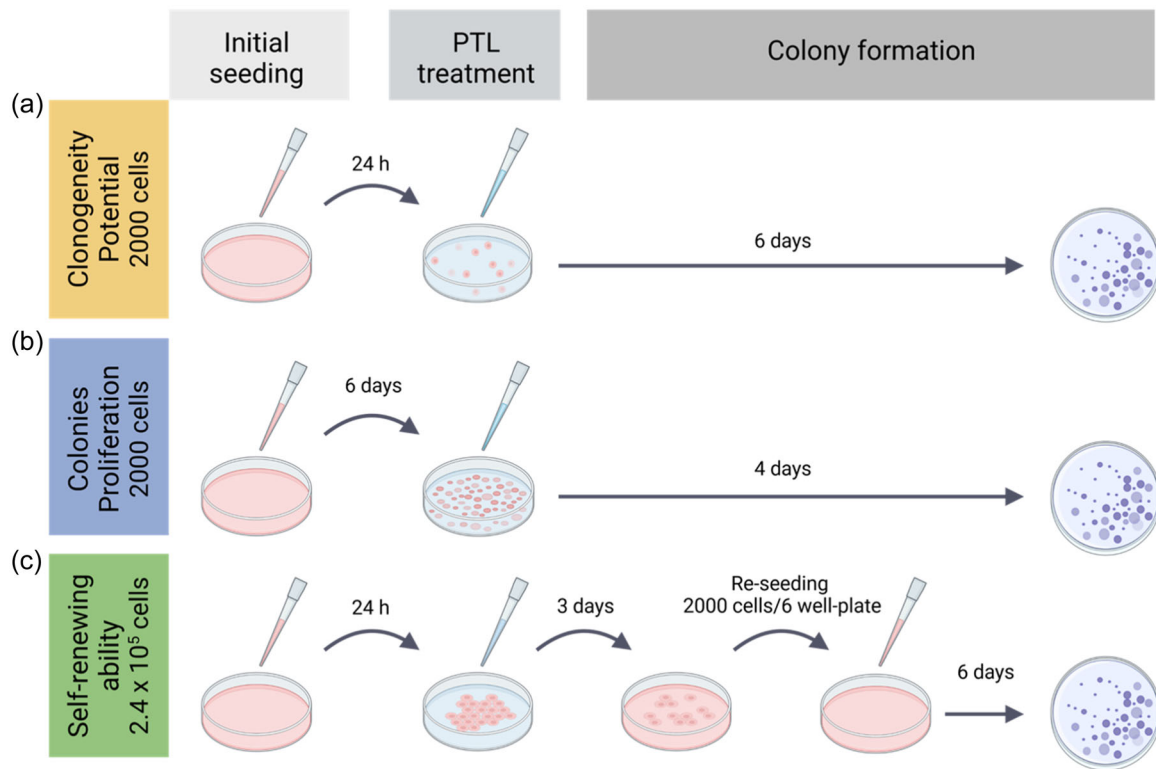
FIGURE 1 Protocols followed for the different experiments concerning colony formation. Briefly, to measure the clonogenicity potential (a), SKOV-3 and OC314 epithelial ovarian cancer (EOC) cells were seeded at low density and, 24 h after seeding, they were treated by plasma-treated liquids (PTLs) and allowed to grow for 6 days. For proliferation measurement (b), EOC cells were also seeded at low density, but this time allowing them to grow for 6 days before treatment plus 4 days after it. To estimate self-renewing ability (c), EOC cells were seeded to reach confluence after 24 h and then they were treated with PTLs. After 3 days of treatment, surviving cells were recovered and re-seeded at low density and allowed to grow for 6 days. At the end point of each experiment, colonies were fixed and stained with crystal violet for their quantification.

To assess self-renewing, SKOV-3 and OC314 were seeded in 24-well plates at the density of 2.4×10^5 cells/well in complete media (Figure 1c). After 24 h, cells were treated with 500 µL of freshly produced PTR and PTRL at 15 and 20 s of plasma gas exposure, or their corresponding UT. After 2 h of treatment, cells were washed with PBS and cultured for 3 days. Afterward, surviving cells were harvested, and 2.000 cells/well were seeded in 6-well plates in complete medium. Colonies were fixed, stained, and analyzed after 6 days, changing the media every 3 days. Colony growth area was quantified by employing ImageJ software. All data were expressed as fold change with respect to UT.

2.7 | Statistical analyses

Statistical analyses were performed using GraphPad Prism software version 8.0. The comparison of means between different groups of numerical variables was performed using two-way analysis of variance (ANOVA) with Geisser–Greenhouse correction. The results were expressed as the mean $\pm$ standard error of the mean (SEM; $n \geq 3$) and statistical significance is specified with asterisks (*$p \leq 0.05$, **$p \leq 0.001$).

3 | RESULTS

3.1 | Chemical characterization of PTLs

To evaluate the influence of the plasma treatment on the reactive species generated in R and RL, the solutions were treated for selected times, from 15 to 300 s, and then analyzed. H_2O_2 and NO_2^- generated due to the treatment were quantified right after exposure (Figure 2a,b). In all cases, the concentration of both species increased linearly with the treatment time. By linear fitting the data, it was possible to obtain the generation rate (v) of both species in PTR and PTRL (reported in the figure). We obtained the same values, within the experimental error, with and without the presence of lactate during the
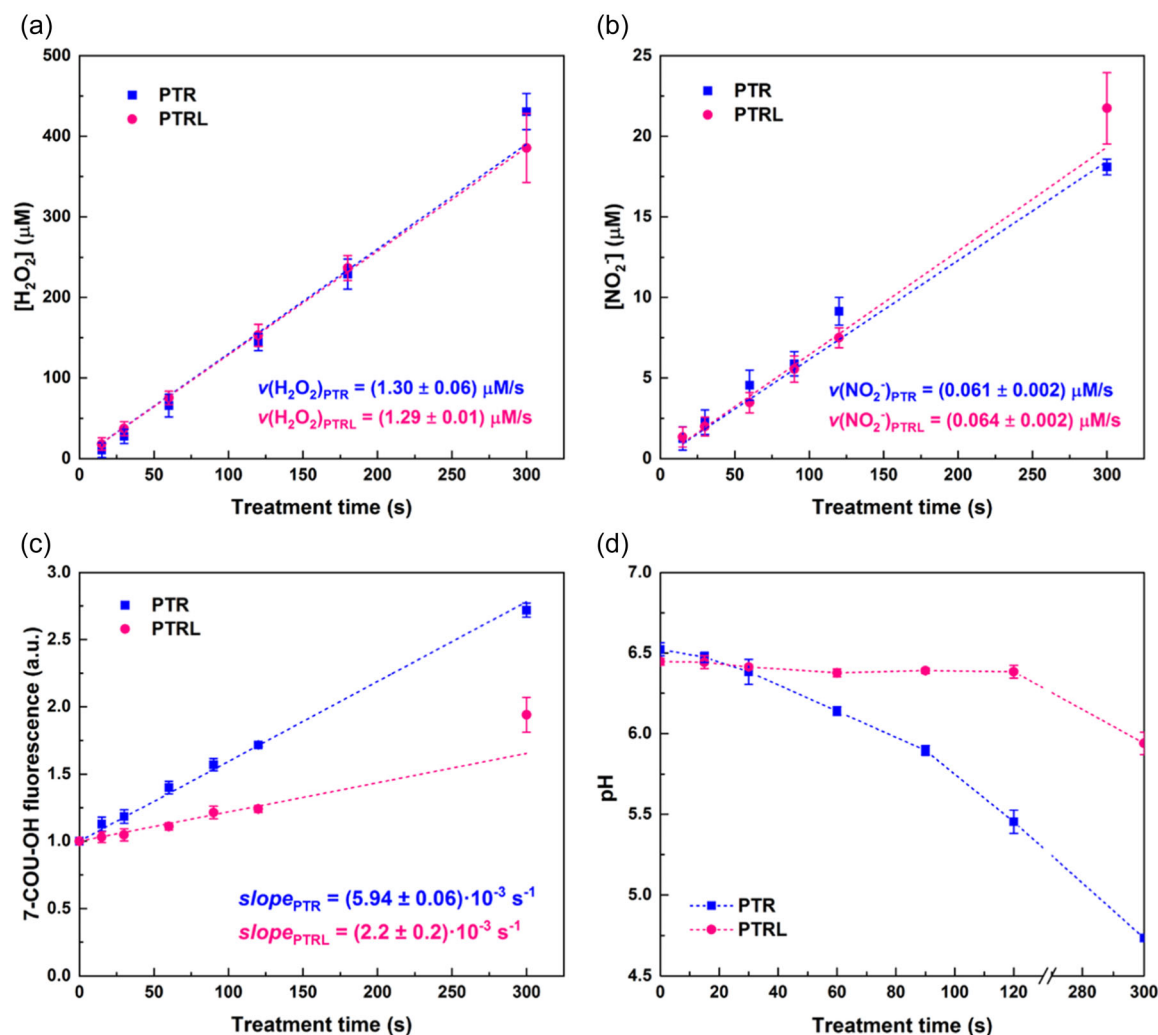
FIGURE 2 Reactive oxygen and nitrogen species in plasma-treated Ringer's saline (PTR) and plasma-treated Ringer's lactate (PTRL) as a function of treatment time. Concentration of H_2O_2 (a) and NO_2^- (b); the dashed lines are the linear interpolations of the experimental data. (c) Fluorescence signal due to the generation of 7-COU-OH in PTR and PTRL containing 1 mM of coumarin as a function of plasma treatment time; the dashed lines are the linear interpolations of the experimental data. (d) pH evolution in PTR and PTRL solution at increasing plasma treatment time. All data are presented as the mean $\pm$ SEM ($n \geq 3$).

treatment, implying that it does not affect the generation of long-lived reactive species.

The production of OH radicals was assessed by adding COU in R and RL during the plasma treatment. Figure 2c reports the fluorescence signals, due to the generation of 7-COU-OH, in PTR and PTRL as a function of the treatment time. The signals increase linearly with the treatment time in both PTR and PTRL. However, a significantly lower rate of OH formation was recorded in the presence of lactate during the treatment.

Figure 2d reports the evolution of pH in PTR and PTRL. Plasma treatment induced a progressive pH decrease from 6.5 to 4.7 in PTR and to 5.9 in PTRL. The difference is due to the buffering properties of the lactic acid/lactate pair ($pK_a = 3.86$).

To assess the impact of plasma treatment on lactate, a 0.5 mM L solution in R was treated by plasma at different times and analyzed with HPLC (Figure 3). In this way, the lactate in the solution and any oxidation product generated during the treatment were separated and detected. The lactate concentration in this experiment was lower than the actual lactate concentration in the other experiments reported in this paper to maximize the effects of the plasma treatment and make them easier to detect and measure. It can be reasonable to assume that the effects measured at this concentration of lactate are the same as those that happen at higher concentration, just to a different extent. Figure 3a reports the region of chromatograms of untreated RL and 6 min PTRL with the peak of lactate (r.t. 2.47 min) obtained by
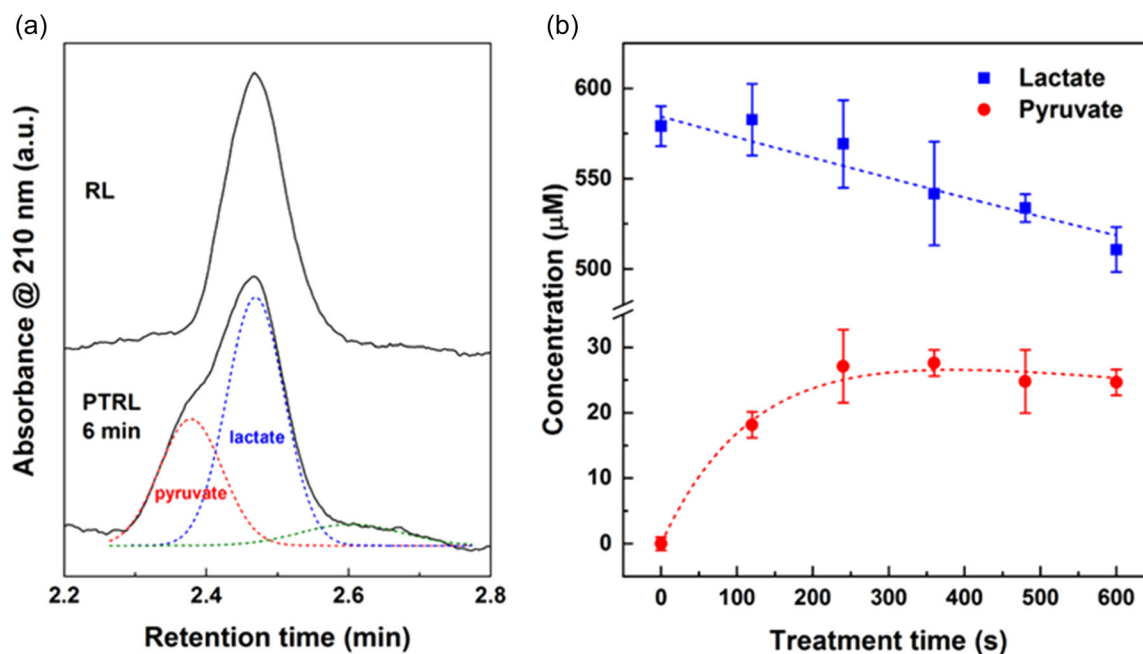
FIGURE 3 (a) Chromatograms of untreated Ringer's lactate and 6 min plasma-treated Ringer's lactate, with a theoretical initial lactate concentration 0.5 mM; the dashed lines correspond to the deconvolution of the high performance liquid chromatography signal using three Gaussian components. (b) Concentration of lactate and pyruvate as a function of the plasma treatment time; the dashed lines are the interpolation of the experimental data using the exponential function ($C = C_0 e^{-k_1 t}$) and peak function ($C = C_0 k_1 \frac{e^{-k_1 t} - e^{-k_2 t}}{k_2 - k_1}$) for lactate and pyruvate, respectively.

deconvolution. By increasing the plasma treatment time, two new peaks appear at r.t. 2.38 and 2.63 min, which are due to the formation of oxidation products. In particular, the peak at 2.38 min was identified as pyruvate, by analyzing a standard pyruvate solution using the same conditions. This is in line with nuclear magnetic resonance spectra reported by Hori et al.[19,56] The peak areas of lactate and pyruvate were obtained by peak deconvolution of the region between 2.2 and 2.8 min and are reported in Figure 3b as a function of the plasma treatment time. As expected, the concentration of lactate decreases with a half-life time of (58 ± 7) min. At the same time, the concentration of pyruvate increases until a maximum is reached around 6 min and then it slowly decreases. This means that pyruvate is generated by the oxidation of lactate, but it is then further oxidized by plasma-generated RONS. To obtain an estimation of the amount of pyruvate generated during the treatment of non diluted RL, we treated this solution and analyzed it using the same procedure (Supporting Information: Figure S1). In that case, due to the very high area of the lactate peak, the isolation of the pyruvate peak was more difficult and we were able to obtain the approximate concentration of pyruvate generated during 5–10 min treatment of non diluted RL to be around 300–400 μM.

3.2 | Effect of PTRL and PTR on EOC cell viability

The metabolic activity on four EOC cell lines, namely SKOV-3, OV-90, OVSAHO, and OC314, was measured employing the WST-1 assay to assess the cytotoxic effect exerted by PTRL and PTR. EOC cells were exposed to PTRL and PTR solutions produced at different plasma treatment times (from 15 to 60 s) and adding 10% FBS after treatment, to restore pH and provide nutrients to cells (Figure 4). The pH after the addition of 10% FBS was checked for each plasma treatment time and no variation from the physiological value was observed. SKOV-3 and OC314 (Figure 4a,b) significantly decreased their viability already with 15 s PTLs and were similarly affected by PTRL and PTR; the cytotoxic effect was fostered 72 h after treatment displaying an evident plasma treatment-time dependence (Supporting Information: Figure S2a,b) and a dramatic decrease in viability over 90% for the conditions at 30 and 60 s.

On the other hand, OV-90 and OVSAHO (Figure 4c,d) showed less sensitivity to the treatments and appeared to be affected only when they were exposed to liquids treated for long times (30 and 60 s). However, these conditions were not sufficient to definitely inhibit
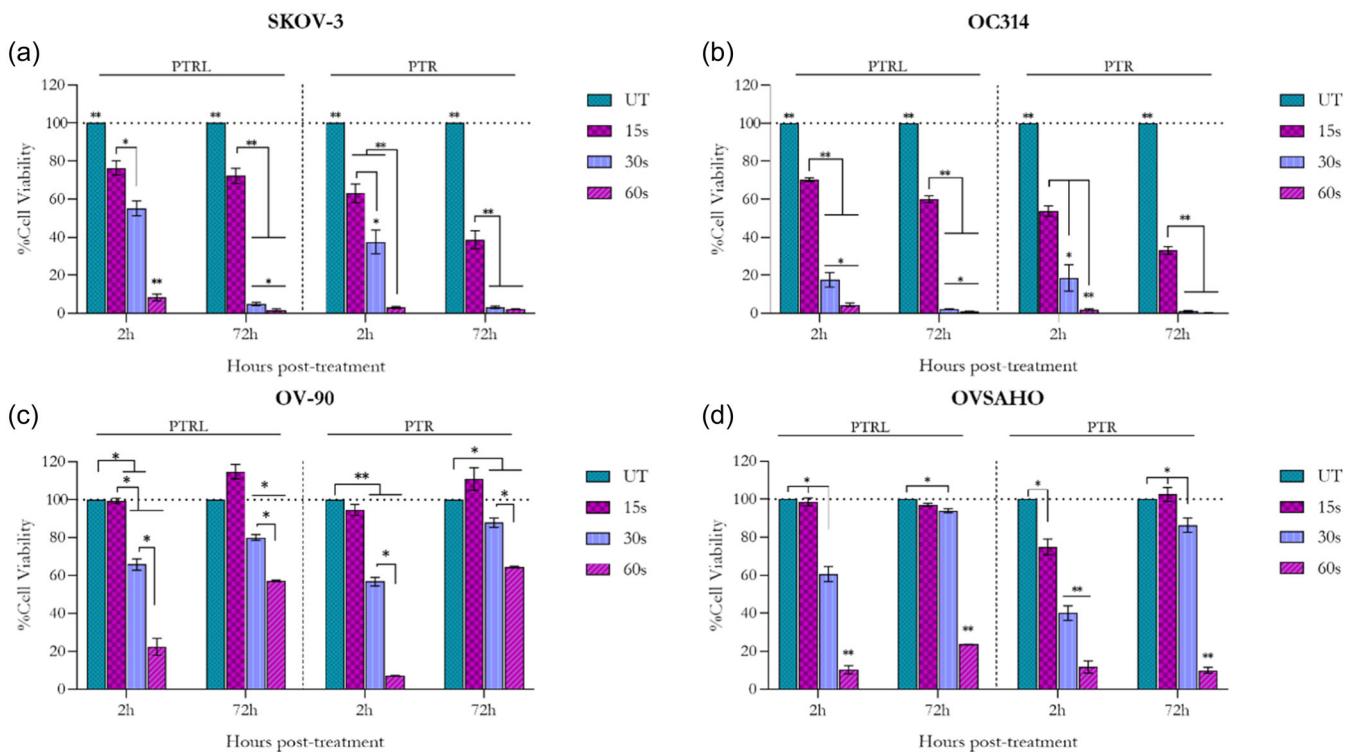
FIGURE 4 Effects of plasma-treated Ringer's lactate (PTRL) and plasma-treated Ringer's saline (PTR) solution on cell viability on epithelial ovarian cancer cell lines. Viability of SKOV-3 (a), OC314 (b), OV-90 (c), and OVSAHO (d) cell cultures treated with PTRL and PTR solutions, produced at different plasma treatment times, at 2 and 72 h after treatment. Cell viability was normalized to the corresponding control (100) at 2 h and plotted as fold change relative to the corresponding untreated control (UT) (Ringer's lactate for PTRL treatments and Ringer's saline for PTR treatments) sample, for both time points. All data are presented as the mean $\pm$ SEM ($n \geq 3$); *$p < 0.05$, **$p < 0.001$.

the cell proliferative capability during the subsequent 72 h, where cells recovered their viability compared to control for OV-90 and showed cytostatic effect at PTLs 60 s. OV-90 cells showed a 20%−40% decrease in cell viability at 72 h from PTL treatment, whereas OVSAHO cell line appeared to suffer the exposure to PTLs 60 s showing a cytostatic effect during the cultured time frame (Supporting Information: Figure S2c,d).

Although PTRL and PTR exerted a similar cytotoxic effect on SKOV-3 and OC314, slightly higher cell viability was detected in PTRL than in PTR. More specifically, SKOV-3 showed a survival rate after 15 s-PTRL and 15 s-PTR of 72% and 38%, respectively, while for treatment at 30 s it was 5% for PTRL and 3% for PTR. OC314 showed the same trend with a cell survival of 60% for 15 s-PTRL and 33% for 15 s-PTR. The treatment at 30 s had a survival rate of 2% for PTRL and 1.2% for PTR. A similar trend but less marked was observed with OV-90 and OVSAHO. This tendency was also confirmed in a 3D scenario, obtained from preliminary confocal microscope images on collagen-based scaffolds seeded with SKOV-3 and OC314 cells to obtain 3D tumor models (Supporting Information: Figure S3).

3.3 | Understanding the effect of lactate on EOC cell viability

At this point, we wanted to evaluate how lactate influences PTLs cytotoxicity and whether this is influenced by plasma treatment. Given the higher cytotoxic effects on SKOV-3 and OC314 due to PTRL and PTR observed in Figure 4, these two cell lines were selected to understand the possible correlation among plasma treatment, presence of lactate, and cell viability (Figure 5a,b). The lower cytotoxic effect found at 20 s plasma treatment (cell survival below than 40% after 72 h exposure to PTLs), compared to the 30 s plasma treatment (less than 10%, Figure 4a,b), abrogates any lactate-induced effect. SKOV-3 and OC314 were exposed to PTR, PTRL and PTR+L for 2 h (Figure 5a,b). Surprisingly, when EOC lines were treated with PTR+L for 15 and 20 s, the cytotoxic effect of PTR on cell viability was significantly reduced, which was evident at 15 s exposure whereby the effect on the EOC growth could be directly compared with the one induced by PTRL. In contrast, 20 s plasma treatment showed significant differences between PTRL and PTR+L.
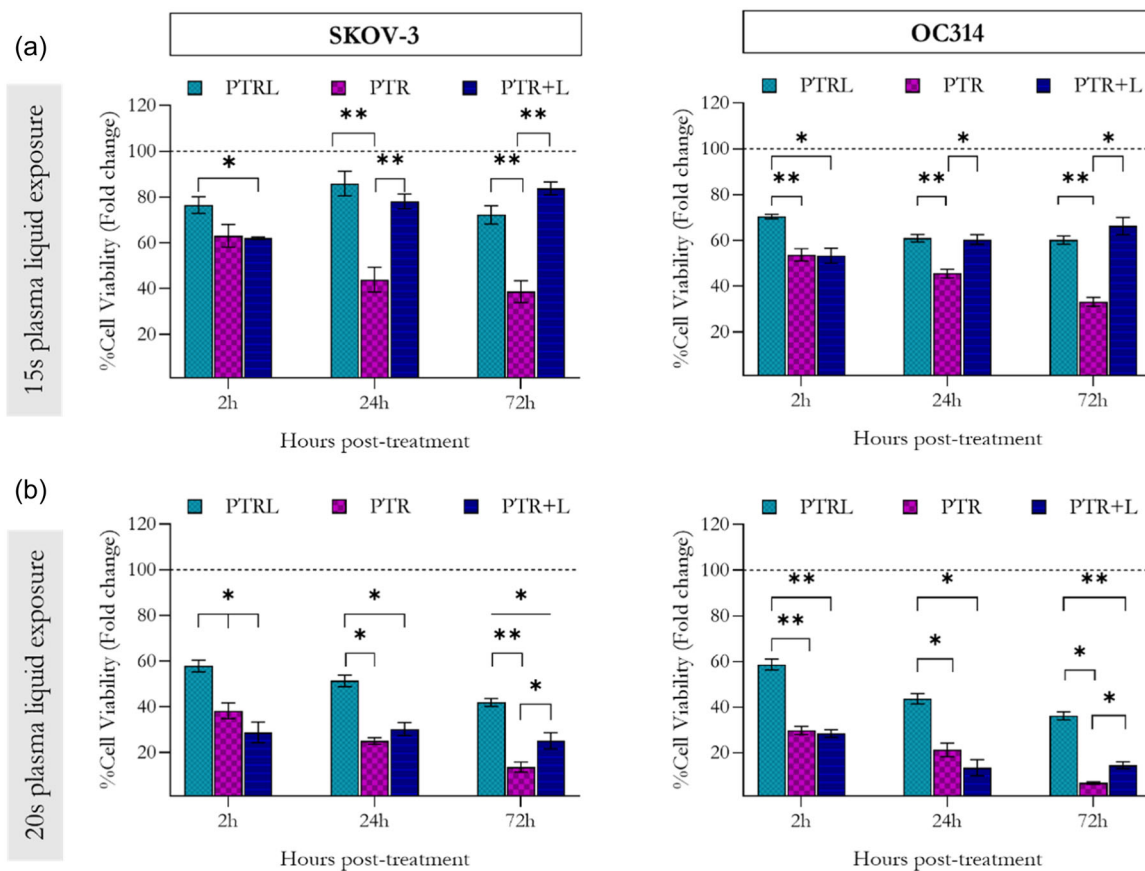
FIGURE 5 Lactate is affected by plasma treatment and reduces the cytotoxicity of plasma-treated liquids (PTLs). Relative viability of cells treated with PTLs produced by exposure to plasma for 15 s (a) and 20 s (b). Cell viability was normalized to the corresponding control at 2 h and plotted as fold change relative to the corresponding untreated control (UT) (Ringer's lactate [RL] for plasma-treated Ringer's lactate [PTRL] treatments, Ringer's saline [R] for PTR treatments, and R + L for plasma-treated Ringer's saline with the addition of lactate post treatment [PTR + L]) sample, for both time points. All data are presented as the mean ± standard error of the mean ($n \geq 3$); *$p < 0.05$, **$p < 0.001$.

More specifically, the presence of lactate in PTR (PTR+L) reduced the PTR cytotoxicity in SKOV-3 by 45% and 10% at 15 and 20 s plasma treatment times, respectively. In OC314 cells, lactate induced a loss of cytotoxicity of 33% and 7% in 15 s- and 20 s-treated PTR+L, respectively.

## 3.4 | Effect of PTRL and PTR on EOC tumorigenic potential

Finally, we attempted to evaluate if PTLs were able to affect the capability of EOC to maintain survival and mitotic ability. Indeed, cancer cells are characterized by the ability to generate colonies of a single cell-derived clonal population and initiate tumorigenesis.[57] As shown in Figure 6a, both PTR and PTRL treatments completely abolished the EOC clonogenicity, in both cell lines and treatment times investigated. In addition, when preformed colonies were treated with PTLs, both EOC

colony populations were severely affected by PTL treatments, with respect to the control, and a significant correlation between the clonal growth and the PTL exposure time was observed (Figure 6b). Overall, PTR and PTRL were able to inhibit the tumorigenic potential and blunted colonies proliferative capability on both EOC cells, in particular with a significant efficacy after 20 s PTLs. These data validated a strict correlation between time-liquid exposure to plasma gas and cell response, apparently independent of the kind of liquid employed.

To ascertain whether PTL treatment may have some influence on EOC aggressiveness, in terms of the capacity of residual tumor cells to form recurrences (Figure 7), the effect of PTR and PTRL solutions was tested on pretreated SKOV-3 and OC314, following the procedure described in Figure 1c. Colony formation results indicate that neither PTR nor PTRL treatments affected the EOC aggressiveness.
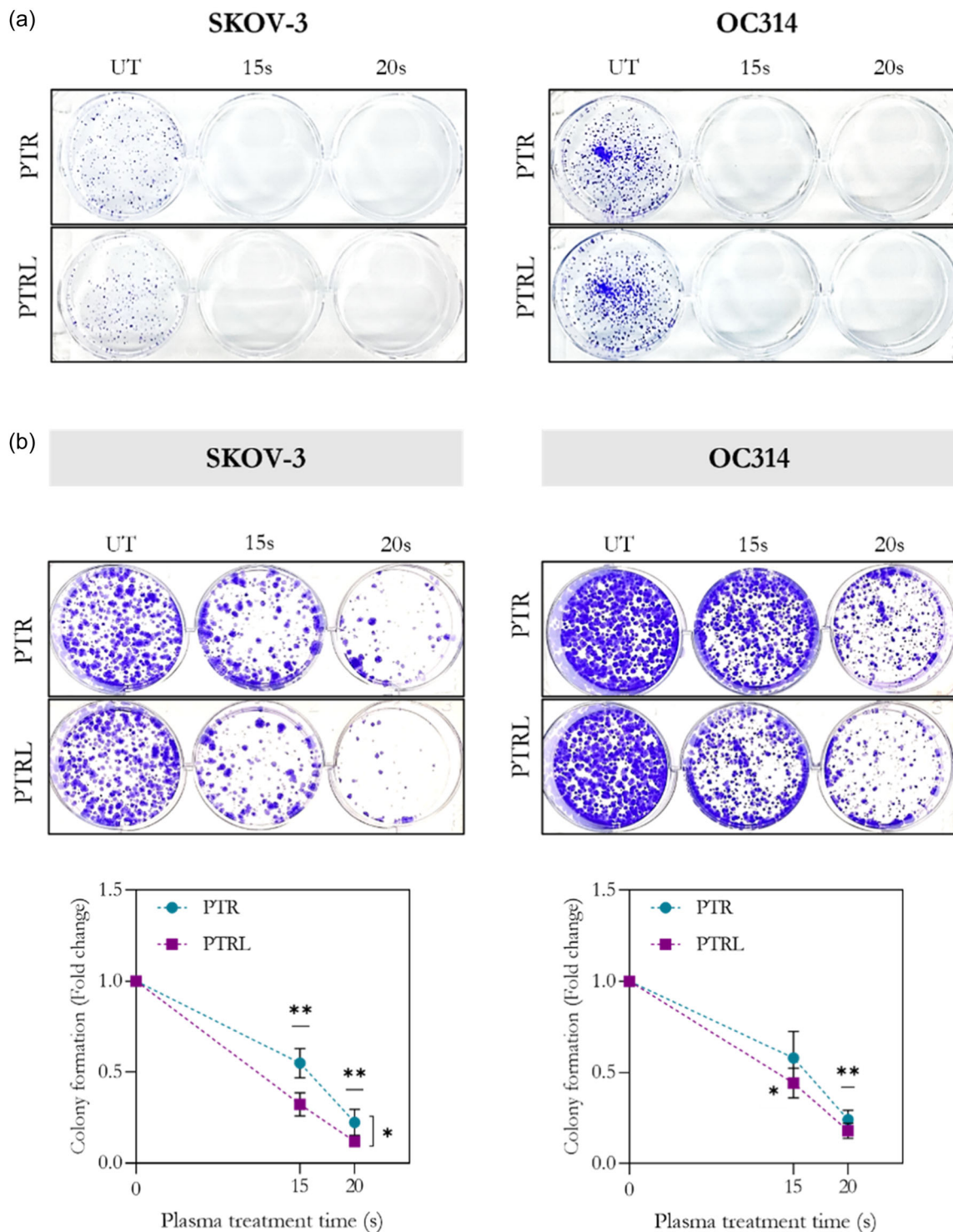
FIGURE 6 Plasma-treated liquid inhibit the clonogenic potential and blunted colonies proliferative capability in epithelial ovarian cancer models. Representative images of 6-well plates containing SKOV-3 and OC314 cells plated at 2.000 cells/well and grown for 6 days (a) and 10 days (b), then stained with crystal violet (CV). CV absorbed by the cells on each plate was released and absorbance at 590 nm was measured on a spectrophotometer. Relative growth curves of treated clones at 10 days were measured (b); absorption measurements were normalized and plotted as fold change relative to the corresponding untreated control (UT) sample. All data are presented as the mean $\pm$ SEM ($n \geq 3$); *$p < 0.05$, **$p < 0.001$.
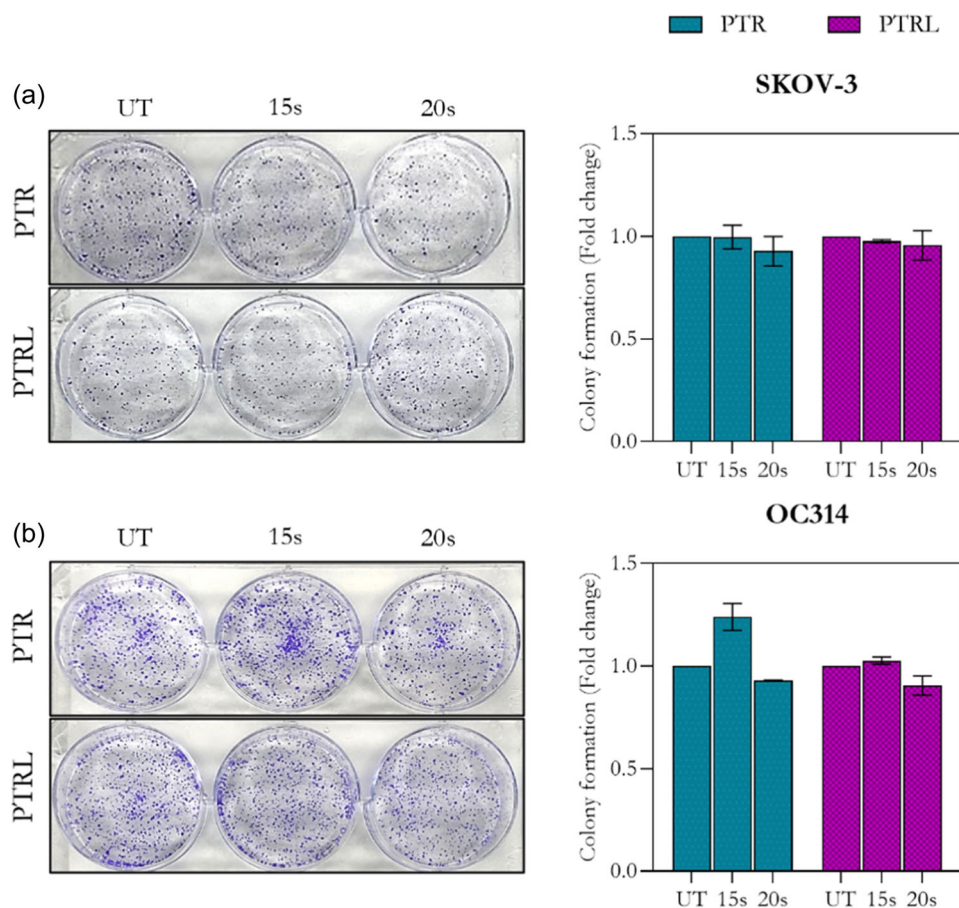
FIGURE 7 Plasma-treated liquids do not exacerbate the epithelial ovarian cancer (EOC) aggressiveness. EOC cells were treated with 15 s and 20 s plasma-treated Ringer's saline (PTR) and plasma-treated Ringer's lactate (PTRL) for 2 h, then cultured for 3 days. The surviving fraction was harvested, plated at 2.000 cells/well in 6-well plates and grown for 6 days. The colonies were stained with crystal violet and photographed. Representative images of the colonies formed for SKOV-3 (a) and OC314 (b). Relative bar graph quantifies the area covered by the colonies and expressed as fold change of the control (UT). Data are presented as the mean $\pm$ SEM ($n = 2$).

4 | DISCUSSION

Several studies have reported the antitumor activity of different liquids that have been exposed to CAP[29,37,39] against several cancer cell lines, promoting apoptosis and inhibiting proliferation.[13,21,32,36,42,56,58] In this work, the effect in EOC cell lines of two clinically relevant solutions, R and RL, exposed to kINPen plasma jet was analyzed. The kINPen plasma source is a certified medical device, which uses argon to produce plasma, extensively characterized in the literature.[50,59] Several applications of kINPen have been reported in the field of plasma medicine.[12,14,60–62] The interaction between plasma, surrounding air and liquid substrates leads to the production of RONS in these liquids.[12]

In both PTR and PTRL, we measured similar amounts of H_2O_2 and NO_2^-, whose concentrations increase linearly with the treatment time (Figure 2a,b). Along with that, a pH decrease in PTLs was observed as a function of treatment time (Figure 2d), because of the reactions among nitrogen species leading to acidification through the formation of nitrous and nitric acid.[63] The drop in pH was less evident in PTRL since lactate acts as a buffer according to the lactate/lactic acid–base equilibrium.[45] The indirect measure of OH radicals by COU probe (Figure 2c) showed a time-dependent formation of OH in PTLs. Notably, the results indicated that the presence of lactate during the treatment influenced the 7-COU-OH signal inducing a slower increase in it, suggesting that lactate acts as a scavenger of OH radicals. Recent studies have reported that CAP treatment induces chemical modifications in RL solution due to the oxidation of lactate to pyruvate by reaction with OH radicals.[56,64] Our HPLC analysis goes in this direction, confirming that the plasma treatment oxidized lactate to pyruvate in PTRL (Figure 3) and a possible chemical pathway involves the participation of OH radicals. However, more experiments would be necessary to confirm this hypothesis.

PTR and PTRL produced by kINPen were supplemented with 10% FBS immediately after plasma treatment to restore physiological pH and avoid its influence on cell response, as previously reported.[39] The PTL dose–response profile on EOC viability was validated, showing higher cytotoxicity induced by PTR than PTRL, ascribed to the presence of lactate and the production of pyruvate during the plasma treatment (Figure 4). Overall, PTRL and PTR exerted a cytotoxic dose–response trend in EOC cells related to the plasma treatment time of the liquid. Specifically, PTLs affected SKOV-3 and OC314 cell viability displaying a time-dependent increase of cytotoxic effect. In contrast, OV-90 and OVSAHO cell lines only appeared to be affected by PTLs initially, as they tended to recover their proliferative capability during the subsequent cultured time.

To maximize its effects and determine its possible role in the cytotoxicity the of PTLs, we added a double concentration of lactate to PTR post treatment (PTR+L) than the present in PTRL. The cytotoxicity of PTR was significantly reduced for longer plasma treatment times but not for shorter ones (Figure 5a,b). This effect may be due to the lactate being affected by long-lived RONS when they are present in sufficient amounts to oxidize it to pyruvate for long plasma treatments. The presence of pyruvate in the PTL could have a cytoprotective effect, attenuating oxidative injury in the cells.[48,49,65] Pyruvate can influence the effectiveness of CAP by protecting cells from the cytotoxic effects of H_2O_2 through several mechanisms.[48] On the one hand, pyruvate can scavenge H_2O_2 at later states through an oxidative decarboxylation reaction, producing CO_2, H_2O, and acetate.[49] This reaction is also important in protecting cells from oxidative stress induced by mitochondria activity, which also contributes to stimulating the cellular antioxidant defense systems to counteract high levels of H_2O_2.[48,66] On the other hand, it has been suggested that the cytotoxic effects of CAP may also be due to a reduction in antioxidant defenses or to the depolarization of the mitochondrial membrane.[48,67,68] To avoid mitochondrial damage and also to increase ATP production, cancer cells are able to switch from oxidative respiration to lactic fermentation, which is known as the Warburg effect.[69] An increase in the available pyruvate may even favor this cytoprotective effect.[70] Therefore, pyruvate is an important factor to consider in understanding the effectiveness of CAP.

Oxidative stress has a major role in many biological processes, such as proliferation and differentiation, while over a certain intracellular level, ROS are responsible for cytotoxic and cytostatic effects.[40] Clonogenicity is one of the most important characteristic features of cancer cells to guarantee both processes. When the effect of PTLs on this cancer hallmark was analyzed, both PTR and PTRL effectively led to an abrogation of the clonogenic capacity and to a strong inhibition of colony proliferative capacity in a dose-dependent manner. This could indicate a potential of the treatment to avoid the effect of tumor burden and aggressiveness, as it is the case in relapses,[71] although this should be confirmed in 3D or in vivo[70] scenarios in future works.

Overall, this study demonstrated that PTR and PTRL exert a strong cytotoxic effect on EOC models, and this is attributable not only to a synergy between CAP-generated RONS but also to additional intermediate molecules that are generated and influenced by CAP-dependent reactions that modulate the different cellular responses. Thus, PTLs have shown to be effective as new possible adjuvant approaches for EOC treatment. Although still far from clinical application, PTLs could represent an opportunity to increase the efficacy of current therapeutic strategies and improve patient outcomes.

5 | CONCLUSIONS

The present study is the first to compare the cytotoxic effect of Ringer's saline and Ringer's lactate solution exposed to physical plasma. This was done in particular by evaluating the effects on four different EOC cell lines. We observed that plasma induced lactate conversion to pyruvate. Pyruvate is known as a key ROS scavenger and metabolic intermediate. Despite the presence of pyruvate in PTRL, just a minor decrease in its biological activity (cytotoxicity and clonogenic potential) was found, PTR tending to be more cytotoxic. In light of the results found, both solutions can be considered as relevant vehicles for plasma-generated RONS and with potential for transfer to the clinics.

AUTHOR CONTRIBUTIONS

Cristiana Bucci was involved in experimental and writing—original draft. Francesco Tampieri was involved in conceptualization and investigation, writing, review, and editing, and Miguel Mateu-Sanz was involved in investigation, writing, review, and editing. Romolo Laurita, Vittorio Colombo, and Cristina Canal were involved in project management, conceptualization, writing, review, and editing.

CONFLICT OF INTEREST STATEMENT

The authors declare no conflict of interest.

DATA AVAILABILITY STATEMENT

The data that support the findings of this study are available from the corresponding author upon reasonable request.

ORCID

Cristiana Bucci https://orcid.org/0000-0003-2528-2609
Francesco Tampieri http://orcid.org/0000-0003-1474-867X
Miguel Mateu-Sanz http://orcid.org/0000-0001-5117-6071
Romolo Laurita http://orcid.org/0000-0003-1744-3329
Vittorio Colombo http://orcid.org/0000-0001-9145-198X
Cristina Canal http://orcid.org/0000-0002-3039-7462

REFERENCES

[1] P. Zheng, P. Zheng, G. Chen, *Front. Med.* **2021**, *8*, 756401.
[2] J. O. A. M. van Baal, C. J. F. van Noorden, R. Nieuwland, K. K. Van de Vijver, A. Sturk, W. J. van Driel, G. G. Kenter, C. A. R. Lok, *J. Histochem. Cytochem.* **2018**, *66*, 67–83.
[3] R. Brett M., P. Jennifer B., S. Thomas A., R. Brett M., P. Jennifer B., S. Thomas A., *Cancer Biol. Med.* **2017**, *14*, 9–32.
[4] S. Lheureux, C. Gourley, I. Vergote, A. M. Oza, *Lancet* **2019**, *393*, 1240–1253.
[5] A. Rynne-Vidal, C. L. Au-Yeung, J. A. Jiménez-Heffernan, M. L. Pérez-Lozano, L. Cremades-Jimeno, C. Bárcena, I. Cristóbal-García, C. Fernández-Chacón, T. L. Yeung, S. C. Mok, P. Sandoval, M. López-Cabrera, *J. Pathol* **2017**, *242*, 140–151.
[6] S. P. Bisch, A. Sugimoto, M. Prefontaine, M. Bertrand, C. Gawlik, S. Welch, J. McGee, *J. Obstet. Gynaecol. Canada* **2018**, *40*1283–1287.e1.
[7] R. Oun, Y. E. Moussa, N. J. Wheate, *Dalt. Trans.* **2018**, *47*, 6645–6653.
[8] C. Della Pepa, G. Tonini, C. Pisano, M. Di Napoli, S. C. Cecere, R. Tambaro, G. Facchini, S. Pignata, *Chin. J. Cancer* **2015**, *34*, 17–27.
[9] A. Jewell, M. McMahon, D. Khabele, *Cancers* **2018**, *10*, 296.
[10] M. Sant, P. Minicozzi, M. Mounier, L. A. Anderson, H. Brenner, B. Holleczek, R. Marcos-Gragera, M. Maynadié, A. Monnereau, G. Osca-Gelis, O. Visser, R. De Angelis, *Lancet Oncol* **2014**, *15*, 931–942.
[11] J. Prat, *J. Gynecol. Oncol* **2015**, *26*, 87.
[12] D. Brány, D. Dvorská, E. Halašová, H. Škovierová, *Int. J. Mol. Sci* **2020**, *21*, 2932.
[13] T. Adachi, Y. Matsuda, R. Ishii, T. Kamiya, H. Hara, *J. Clin. Biochem. Nutr.* **2020**, *67*, 232–239.
[14] A. Privat-Maldonado, A. Schmidt, A. Lin, K.-D. Weltmann, K. Wende, A. Bogaerts, S. Bekeschus, *Oxid. Med. Cell. Longev.* **2019**, *2019*, 1–29.
[15] T. Von Woedtke, A. Schmidt, S. Bekeschus, K. Wende, K.-D. Weltmann, *In Vivo* **2019**, *33*, 1011–1026.
[16] D. B. Graves, *Plasma Process. Polym* **2014**, *11*, 1120–1127.
[17] D. B. Graves, *J. Phys. D. Appl. Phys.* **2012**, *45*, 263001.
[18] M. Gherardi, E. Turrini, R. Laurita, E. De Gianni, L. Ferruzzi, A. Liguori, A. Stancampiano, V. Colombo, C. Fimognari, *Plasma Process. Polym.* **2015**, *12*, 1354–1363.
[19] H. Tanaka, K. Nakamura, M. Mizuno, K. Ishikawa, K. Takeda, H. Kajiyama, F. Utsumi, F. Kikkawa, M. Hori, *Sci. Rep.* **2016**, *6*, 36282.
[20] K. Nakamura, Y. Peng, F. Utsumi, H. Tanaka, M. Mizuno, S. Toyokuni, M. Hori, F. Kikkawa, H. Kajiyama, *Sci. Rep.* **2017**, *7*, 6085.
[21] Y. Sato, S. Yamada, S. Takeda, N. Hattori, K. Nakamura, H. Tanaka, M. Mizuno, M. Hori, Y. Kodera, *Ann. Surg. Oncol.* **2018**, *25*, 299–307.
[22] S. Nijdam, E. van Veldhuizen, P. Bruggeman, U. Ebert, An Introduction to Nonequilibrium Plasmas at Atmospheric Pressure in Plasma Chemistry and Catalysis in Gases and Liquids (Edd. V. I. Parvulescu, M. Magureanu, P. Lukes), Wiley-VCH Verlag & Co. KGaA, Weinheim **2012**.
[23] B. R. Locke, P. Lukes, J. L. Brisset, Elementary Chemical and Physical Phenomena in Electrical Discharge Plasma in Gas–Liquid Environments and in Liquids in Plasma Chemistry and Catalysis in Gases and Liquids (Edd. V. I. Parvulescu, M. Magureanu, P. Lukes), Wiley-VCH Verlag & Co. KGaA, Weinheim **2012**.
[24] G. Bauer, D. Sersenová, D. B. Graves, Z. Machala, *Sci. Rep.* **2019**, *9*, 14210.
[25] R. J. DeBerardinis, N. S. Chandel, *Sci. Adv.* **2016**, *2*, e1600200.
[26] M. Schieber, N. S. Chandel, *Curr. Biol.* **2014**, *24*, R453–R462.
[27] K. Anam, R. Nasuno, H. Takagi, *Sci. Rep.* **2020**, *10*, 6015.
[28] X. Lu, G. V. Naidis, M. Laroussi, S. Reuter, D. B. Graves, K. Ostrikov, *Phys. Rep.* **2016**, *630*, 1–84.
[29] M. Laroussi, *Front. Phys* **2020**, *8*, 1–7.
[30] A. Weidinger, A. Kozlov, *Biomolecules* **2015**, *5*, 472–484.
[31] B. Farhood, M. Najafi, E. Salehi, N. Hashemi Goradel, M. S. Nashtaei, N. Khanlarkhani, K. Mortezaee, *J. Cell. Biochem.* **2019**, *120*, 71–76.
[32] A. Bisag, C. Bucci, S. Coluccelli, G. Girolimetti, R. Laurita, P. De Iaco, A. M. Perrone, M. Gherardi, L. Marchio, A. M. Porcelli, V. Colombo, G. Gasparre, *Cancers (Basel)* **2020**, *12*, 476.
[33] B. W. L. Lee, P. Ghode, D. S. T. Ong, *Redox Biol* **2019**, *25*, 101056.
[34] M. G. Vander Heiden, R. J. DeBerardinis, *Cell* **2017**, *168*, 657–669.
[35] N. Nguyen, H. Park, S. Hwang, J.-S. Lee, S. Yang, *Appl. Sci.* **2019**, *9*, 801.
[36] T. Matsuzaki, A. Kano, T. Kamiya, H. Hara, T. Adachi, *Arch. Biochem. Biophys.* **2018**, *656*, 19–30.

[37] E. Freund, K. R. Liedtke, R. Gebbe, A. K. Heidecke, L.-I. Partecke, S. Bekeschus, *IEEE Trans. Radiat. Plasma Med. Sci.* **2019**, *3*, 588–596.

[38] N. K. Kaushik, B. Ghimire, Y. Li, M. Adhikari, M. Veerana, N. Kaushik, N. Jha, B. Adhikari, S.-J. Lee, K. Masur, T. von Woedtke, K.-D. Weltmann, E. H. Choi, *Biol. Chem.* **2018**, *400*, 39–62.

[39] M. Mateu-Sanz, J. Tornín, B. Brulin, A. Khlyustova, M.-P. Ginebra, P. Layrolle, C. Canal, *Cancers (Basel)* **2020**, *12*, 227.

[40] E. Turrini, R. Laurita, A. Stancampiano, E. Catanzaro, C. Calcabrini, F. Maffei, M. Gherardi, V. Colombo, C. Fimognari, *Oxid. Med. Cell. Longev.* **2017**, *2017*, 1–13.

[41] J. Ikeda, H. Tanaka, K. Ishikawa, H. Sakakita, Y. Ikehara, M. Hori, *Pathol. Int.* **2018**, *68*, 23–30.

[42] M. Mateu-Sanz, M.-P. Ginebra, J. Tornín, C. Canal, *Free Radic. Biol. Med.* **2022**, *189*, 32–41.

[43] P. L. Marino, *The ICU Book*, 3rd ed., Lippincott Williams & Wilkins, Philadelphia **2007**.

[44] X. Li, Y. Yang, B. Zhang, X. Lin, X. Fu, Y. An, Y. Zou, J.-X. Wang, Z. Wang, T. Yu, *Signal Transduct. Target. Ther.* **2022**, *7*, 305.

[45] S. Singh, C. C. Kerndt, D. Davis, *Ringer's Lactate*, StatPearls Publishing, Treasure Island **2023**.

[46] L. B. Gladden, *J. Physiol* **2004**, *558*, 5–30.

[47] F. Hirschhaeuser, U. G. A. Sattler, W. Mueller-Klieser, *Cancer Res* **2011**, *71*, 6921–6925.

[48] J. Tornin, M. Mateu-Sanz, A. Rodríguez, C. Labay, R. Rodríguez, C. Canal, *Sci. Rep.* **2019**, *9*, 10681.

[49] C. Bergemann, H. Rebl, A. Otto, S. Matschke, B. Nebe, *Plasma Process. Polym.* **2019**, *16*, 1900088.

[50] S. Reuter, T. von Woedtke, K.-D. Weltmann, *J. Phys. D. Appl. Phys.* **2018**, *51*, 233001.

[51] G. Eisenberg, *Ind. Eng. Chem. Anal. Ed.* **1943**, *15*, 327–328.

[52] J. Tornin, C. Labay, F. Tampieri, M.-P. Ginebra, C. Canal, *Nat. Protoc.* **2021**, *16*, 2826–2850.

[53] Y. Nosaka, A. Y. Nosaka, *J. Phys. Chem. C* **2019**, *123*, 20682–20684.

[54] F. Tampieri, M.-P. Ginebra, C. Canal, *Anal. Chem.* **2021**, *93*, 3666–3670.

[55] J. Tornín, A. Villasante, X. Solé-Martí, M.-P. Ginebra, C. Canal, *Free Radic. Biol. Med.* **2021**, *164*, 107–118.

[56] D. Ito, N. Iwata, K. Ishikawa, K. Nakamura, H. Hashizume, C. Miron, H. Tanaka, H. Kajiyama, S. Toyokuni, M. Mizuno, M. Hori, *Appl. Phys. Express* **2022**, *15*, 056001.

[57] V. Rajendran, M. V. Jain, In Vitro Tumorigenic Assay: Colony Forming Assay for Cancer Stem Cells in Cancer Stem Cells, *Methods in Molecular Biology*, 1692 (Eds. G. Papaccio, V. Desiderio), Humana Press, New York **2018**.

[58] F. Utsumi, H. Kajiyama, K. Nakamura, H. Tanaka, M. Mizuno, K. Ishikawa, H. Kondo, H. Kano, M. Hori, F. Kikkawa, *PLoS One* **2013**, *8*, e81576.

[59] S. Bekeschus, A. Schmidt, K.-D. Weltmann, T. von Woedtke, *Clin. Plasma Med* **2016**, *4*, 19–28.

[60] M. Schuster, C. Seebauer, R. Rutkowski, A. Hauschild, F. Podmelle, C. Metelmann, B. Metelmann, T. von Woedtke, S. Hasse, K.-D. Weltmann, H.-R. Metelmann, *J. Cranio-Maxillofacial Surg* **2016**, *44*, 1445–1452.

[61] S. Bekeschus, J. Moritz, I. Helfrich, L. Boeckmann, K.-D. Weltmann, S. Emmert, H.-R. Metelmann, I. Stoffels, T. von Woedtke, *Appl. Sci.* **2020**, *10*, 1971.

[62] L. Miebach, E. Freund, R. Clemen, K.-D. Weltmann, H.-R. Metelmann, T. von Woedtke, T. Gerling, K. Wende, S. Bekeschus, *Free Radic. Biol. Med.* **2022**, *180*, 210–219.

[63] G. Neretti, F. Tampieri, C. A. Borghi, P. Brun, R. Cavazzana, L. Cordaro, E. Marotta, C. Paradisi, P. Seri, M. Taglioli, B. Zaniol, M. Zuin, E. Martines, *Plasma Process. Polym.* **2018**, *15*, 1800105.

[64] Y. Liu, K. Ishikawa, C. Miron, H. Hashizume, H. Tanaka, M. Hori, *Plasma Sources Sci. Technol* **2021**, *30*, 04LT03.

[65] V. A. Guarino, W. M. Oldham, J. Loscalzo, Y.-Y. Zhang, *Sci. Rep.* **2019**, *9*, 19568.

[66] N. K. Kaushik, N. Kaushik, D. Park, E. H. Choi, *PLoS One* **2014**, *9*, e103349.

[67] H. J. Ahn, K. Il Kim, G. Kim, E. Moon, S. S. Yang, J.-S. Lee, *PLoS One* **2011**, *6*, e28154.

[68] K. Panngom, K. Y. Baik, M. K. Nam, J. H. Han, H. Rhim, E. H. Choi, *Cell Death Dis* **2013**, *4*, e642.

[69] M. V. Liberti, J. W. Locasale, *Trends Biochem. Sci.* **2016**, *41*, 211–218.

[70] J. Lu, M. Tan, Q. Cai, *Cancer Lett* **2015**, *356*, 156–164.

[71] K. Santos-de-Frutos, N. Djouder, *Commun. Biol* **2021**, *4*, 747.

SUPPORTING INFORMATION

Additional supporting information can be found online in the Supporting Information section at the end of this article.